

See discussions, stats, and author profiles for this publication at: <https://www.researchgate.net/publication/44800765>

# The aromatic 8-electron cubic silicon clusters Be@Si<sub>8</sub>, B@Si 8 +, and C@Si<sub>8</sub> 2+

ARTICLE *in* THE JOURNAL OF PHYSICAL CHEMISTRY A · JULY 2010

Impact Factor: 2.69 · DOI: 10.1021/jp103180y · Source: PubMed

---

CITATIONS

17

READS

34

## 2 AUTHORS:



Vu Thi Ngan

Quy Nhon University

32 PUBLICATIONS 558 CITATIONS

[SEE PROFILE](#)



Minh Tho Nguyen

University of Leuven

748 PUBLICATIONS 10,835 CITATIONS

[SEE PROFILE](#)

# The Aromatic 8-Electron Cubic Silicon Clusters Be@Si<sub>8</sub>, B@Si<sub>8</sub><sup>+</sup>, and C@Si<sub>8</sub><sup>2+</sup>

Vu Thi Ngan<sup>†,‡</sup> and Minh Tho Nguyen<sup>\*,§</sup>

Department of Chemistry, and Institute for Nanoscale Physics and Chemistry (INPAC), Katholieke Universiteit Leuven, B-3001 Leuven, Belgium, Faculty of Chemistry, National University of Education, Hanoi, Vietnam, and Institute for Computational Science and Technology of HoChiMinh City, Vietnam

Received: April 8, 2010; Revised Manuscript Received: May 24, 2010

The geometrical and electronic structures of the Si<sub>8</sub><sup>2-</sup> dianion and isovalent silicon clusters doped by main second-row elements including Li@Si<sub>8</sub><sup>-</sup>, Be@Si<sub>8</sub>, B@Si<sub>8</sub><sup>+</sup>, C@Si<sub>8</sub><sup>2+</sup>, N@Si<sub>8</sub><sup>3+</sup>, and O@Si<sub>8</sub><sup>4+</sup>, are investigated using quantum chemical methods. The analyses of phenomenological shell model (PSM) combined with partial electron localizability indicators (pELI-D) rationalize the existence of cubic silicon clusters. A cubic cluster can be formed, in the cases of Be@Si<sub>8</sub>, B@Si<sub>8</sub><sup>+</sup>, and C@Si<sub>8</sub><sup>2+</sup>, when three conditions are satisfied, namely, a full occupancy of electronic shells (34 electrons), a presence of positive charge at the center, and a type of spherical aromaticity. A chemical bonding picture for the cubic cage of the doped silicon clusters is illustrated. Each Si atom has four lobes of sp<sup>3</sup> hybridization in which three lobes make three covalent  $\sigma$  bonds with other Si atoms, and the fourth lobe makes a chemical bond with the dopant. The eight delocalized electrons distributed on the fourth lobes describing the bonding between dopant and Si cage follow the Hirsch rule. We demonstrate that a way of applying electron counting rule is to take into account delocalized electrons on the shell orbitals with  $N > 1$  (2S and 2P shell orbitals).

## Introduction

Although silicon clusters (Si<sub>n</sub>) exhibit a diversity of 3-dimensional shapes, a cubic form has not been found to be stable in their small sizes. Whereas the lighter congener C<sub>8</sub>H<sub>8</sub> (cubane) is well-known for chemists, the octasilacubane Si<sub>8</sub>H<sub>8</sub> possessing a cubic structure has never been synthesized.<sup>1</sup> Instead, a C<sub>2</sub> symmetry structure was reported to be the most stable isomer of Si<sub>8</sub>H<sub>8</sub> by using a genetic algorithm coupled with a tight-binding potential to describe the energies of clusters.<sup>1</sup>

Si<sub>8</sub>, the smallest cluster that could possibly exist as a cube, has in fact a C<sub>2h</sub> bicapped octahedral structure, where the two capping atoms are situated at the opposite faces of the octahedron.<sup>2</sup> The Si<sub>8</sub><sup>+</sup> cation favors an edge-capped pentagonal bipyramidal shape.<sup>3</sup> However, it is known that a cluster structure can basically be changed following doping. In this context, a legitimate question is as to whether a cubic silicon cluster could be formed with the presence of a dopant.

Let us first consider the energy levels of a particle in a cubic box. It is well-known that the allowed energies of a particle confined to a cube with infinitely strong walls can be expressed in terms of quantum numbers as follows:  $E = E_0 (N_x^2 + N_y^2 + N_z^2)$ .<sup>4</sup> When quantum numbers N<sub>x</sub>, N<sub>y</sub> and N<sub>z</sub> vary each from 1 to 3, their successive combination leads to nine lowest-energy levels with different degeneracies of 1, 3, 3, 3, 1, 6, 3, 3, 1. Although this sequence is obtained when the potential energy is supposed to be equal to zero within the box and infinite outside the box (a potential being too far from the real potential energy of a molecular system), this suggests that if considering each one-particle state in a cubic environment as an orbital, a closed electron shell can be obtained by filling 22 or 34 or 40... electrons. In the simplest Si<sub>8</sub> species, 32 valence electrons are

available. In a cubic geometry, its actual degenerate HOMO is not completely filled, and a strong Jahn–Teller distortion is thus expected to occur. The corresponding orbital shell could indeed be fully filled by 34 (or 40) electrons; and its full occupancy by an appropriate dopant, which delivers 2 additional electrons, could lead to stable cubic species.

During the course of our study on the doped silicon clusters,<sup>5</sup> we tested this hypothesis and found a few genuine silicon cubes. Recently, Fan et al.<sup>6</sup> reported that the smallest size of the silicon Si<sub>n</sub> cage for a Be atom to be encapsulated in is a cube, with n = 8. Our results are in line with this finding, showing that the Be@Si<sub>8</sub> species constitutes a new and interesting structural feature of the doped silicon clusters. Earlier, insertion of a Be atom inside a Sn<sub>8</sub> cube was also found.<sup>7</sup> However the former authors<sup>6</sup> have not considered the factors that actually stabilize such a small and strained cage. This lack of consideration prompts us to report in this article a detailed analysis of the geometrical and electronic structure to understand its unexpected stability. The scope of our study is also expanded to the other second-row main group elements, ranging from Li to O as dopants, with suitable charges, to give rise to 34 valence electrons, and for which the cube exists.

## Theoretical Approaches

We first apply the phenomenological shell model (PSM), which has been successfully used to explain and predict the magic metallic<sup>8,9</sup> and bimetallic clusters.<sup>10–12</sup> The main assumption of this model is that the delocalized electrons of a cluster move in an average potential that confines them according to the cluster shape. Those electrons are considered as a nearly free electron gas that is contributed by the valence electrons in the case of alkaline and alkaline earth metals. For spherical clusters, the confining potential gives rise to spherical shell of molecular orbitals, whose shapes are similar to the shapes of dominant atomic orbitals. Therefore, the shells of molecular orbitals involved (called shell orbitals) are denoted by capital

\* To whom correspondence should be addressed. E-mail: minh.nguyen@chem.kuleuven.be.

<sup>†</sup> Katholieke Universiteit Leuven.

<sup>‡</sup> National University of Education.

<sup>§</sup> Institute for Computational Science and Technology.

letters S, P, D, F, G,... that actually correspond to the angular momentum quantum number  $L = 0, 1, 2, 3, 4, \dots$  respectively. For a given quantum number  $L$ , the lowest shell orbital has the principle quantum number  $N = 1$ . A normal sequence of phenomenological shell orbitals in a spherical potential is 1S, 1P, 1D, 2S, 1F, 2P, 1G, 2D, 3S,... However, the energy ordering of the shell orbitals can be changed according to the specific potential, which is determined by both the shape and charge of the cluster considered. For binary clusters, the nature of elements also plays an important role in this orbital ordering. Hence, the shell model needs to be carefully applied in each specific case by inspecting the relevant molecular orbitals that can be generated from an ab initio electronic wave function calculation. According to the PSM, the clusters having a closed electronic shell of  $1S^2$ ,  $1S^21P^6$ ,  $1S^21P^61D^{10}$ ,  $1S^21P^61D^{10}2S^2$ ... are expected to be more stable than their neighbors. They can also be referred to the 2-, 8-, 18-, or 20-electron rules in the simpler electron counting rules.

In the case of nonmetal clusters such as those of the group IVA, the electron counting rule has also been employed to interpret the magic clusters. For example, Reveles et al.<sup>13</sup> showed that the stability of transition metal doped silicon clusters can be rationalized on the basis of electron counting rules, in which each Si, which binds to the metal, contributes one valence electron. The systems where the total number of electrons is 20 (in species such as  $ScSi_{16}^-$ ,  $TiSi_{16}$ , and  $VSi_{16}^+$ ,...) seem to exhibit an enhanced stability. The 18-electron rule was often used to interpret the magic cluster  $W@Si_{12}$ , where the W atom resides in a hexagonal prism of  $Si_{12}$ .<sup>14</sup> To examine the validity of the 18-electron rule, Khanna et al.<sup>15</sup> applied it to the case of  $Cr@Si_{12}$ . However, it was not entirely clear if its enhanced stability is actually due to the 18 electrons, or rather due to a 4-fold coordination of Si. Hence, it is still vague about the effective participating electrons of the Si atom. A question of interest is about which electron should be counted to the nearly free electron gas in the case of Si, and how the bonds are made in Si clusters. In the Discussion, we report a solid evidence for taking all of the four valence electrons of each Si atom to the electron gas status of the molecule in order to apply the PSM. Accordingly, we suggest a convenient way of counting the strongly delocalized electrons in doped silicon clusters as in the simpler electron counting rule.

Another approach we use to probe the chemical bonding is the electron localizability indicator (ELI-D)<sup>16</sup> and its orbital decomposition,<sup>17</sup> which have been valuable tools to examine the chemical bonding in transition metal compounds.<sup>18,19</sup> The ELI-D has a simple physical meaning: it measures the fraction of number of electrons necessary to form the given (same) fraction of the same spin electron pairs in each microcell. It can be shown that the ELI-D is proportional to the electron density. As in the case of single determinantal wave functions, the electron density is a sum of orbital densities, ELI-D can thus be decomposed into molecular orbital contributions. These contributions are called partial electron localizability indicators (pELI-D). The ELI-D and pELI-D isosurfaces are computed using the DGrid-4.2 program suite.<sup>20</sup>

Geometrical parameters of the clusters considered are fully optimized using density functional theory calculations with the hybrid functional B3LYP,<sup>21,22</sup> and pure functional BP86,<sup>23,24</sup> and in conjunction with the polarization plus diffuse 6-311+G(d) basis set. Although the former was widely applied for main group element compounds, the latter functional has proved to provide us with reliable geometries of doped silicon clusters.<sup>5</sup> The two functionals give in fact similar results on relative

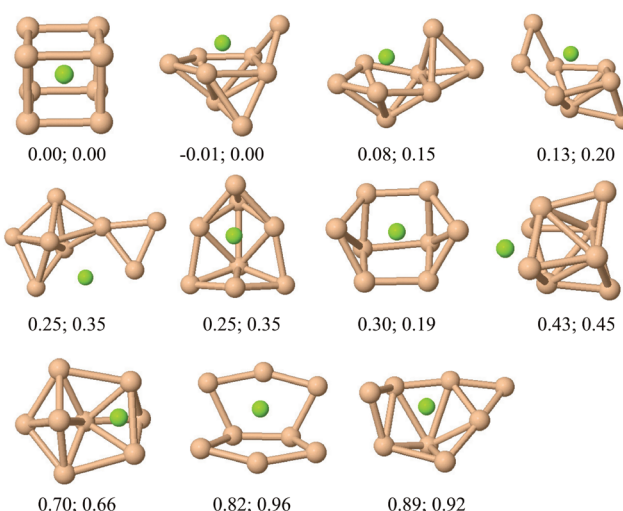


**Figure 1.** Low-lying isomers of  $BeSi_8$  (green ball is Be). Relative energies (eV) are obtained at the B3LYP/6-311+G(d) (left) and BP86/6-311+G(d) (right) levels.

energies of different isomeric forms. However, the B3LYP systematically predicts larger frontier orbital energy gaps than the BP86 for the cubic systems considered. The Gaussian 03 package is used for standard quantum chemical calculations.<sup>25</sup> Harmonic vibrational frequency calculation at the same level is carried out to characterize a stationary point as a local minimum or a transition structure (TS). It has been shown that the ELI-D calculated from Kohn–Sham orbitals at least possesses a similar level of quality as those derived from HF orbitals.<sup>17</sup> Thus, the Kohn–Sham orbitals obtained from BP86/6-311+G(d) densities are used for the orbital analyses.

## Results and Discussion

**Low-lying Isomers of the 34-Electron Systems:  $MSi_8$  ( $M = Li, Be, B, C, N, O$ ) and  $Si_8^{2-}$ .** A search procedure to cover as many as possible atomic arrangements is employed. In particular, all the structures available for doped silicon clusters  $MSi_8$  in the literature are taken as initial geometric configurations. In addition, initial structures are further created by replacing one Si atom in the lower-lying  $Si_8$  isomers by the dopant atom, or by adding a dopant atom to different sites of  $Si_8$  isomers. All the calculations are performed for the lowest-lying electronic singlet state with suitable charges giving rise to a total number of 34 valence electrons.

Our calculations show that the cubic forms of the  $Li@Si_8^-$ ,  $Be@Si_8$ ,  $B@Si_8^+$ ,  $C@Si_8^{2+}$ ,  $N@Si_8^{3+}$ , and  $O@Si_8^{4+}$  clusters are all genuine energy minima. However, only in the case of Be, B, and C dopants, the cube is the lowest-lying isomer. In other cases, the cube is rather local minimum. Figures 1–3 illustrate the low-lying isomers of the  $BeSi_8$ ,  $BSi_8^+$ , and  $CSi_8^{2+}$  clusters, respectively. It should be emphasized that either  $BeSi_8$  or  $CSi_8^{2+}$  has many isomers whose energies are close to that of the cubic structure. The results obtained using both functionals show that each cluster has one isomer which is quasi-degenerate with the cubic isomer, and also a few other isomers having small relative energies. This indicates that the basketlike isomers can coexist with the cubic structure. In contrast, the cubic structure of  $BSi_8^+$  is much energetically lower than other isomers, which implies that the  $B@Si_8^+$  cube can be obtained with high selectivity. This is the recommended cluster to be tested by experiment for a characterization of the cubic shape. The different energetic status of the cubic isomer leads us to the

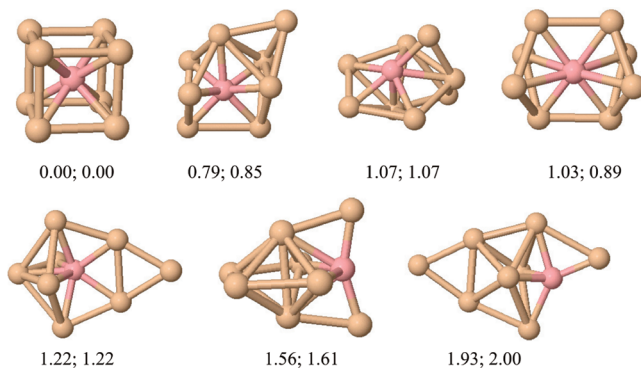


**Figure 2.** Low-lying isomers of  $\text{BSi}_8^+$  (pink ball is B). Relative energies (eV) are obtained at the B3LYP/6-311+G(d) (left) and BP86/6-311+G(d) (right) levels.

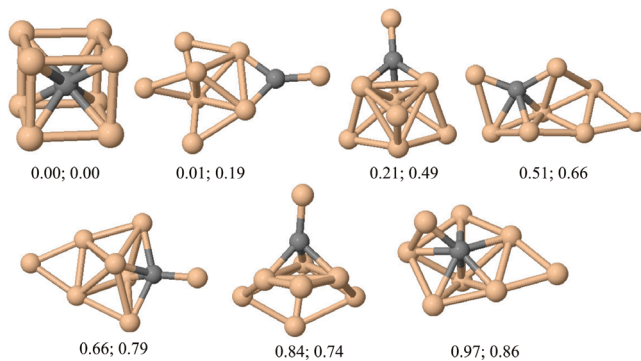


**Figure 3.** Low-lying isomers of  $\text{CSi}_8^{2+}$  (gray ball is C). Relative energies (eV) are obtained at the B3LYP/6-311+G(d) (left) and BP86/6-311+G(d) (right) levels.

question about the necessary and sufficient conditions for the existence of a stable cube.

Relative stability of the cubes can further be confirmed by the positive values of embedding energy (EE) given in the last column of Table 1. This energetic quantity is defined as the energy released upon doping an atom or ion with suitable atomic charge ( $M^n$ ) to the  $\text{Si}_8$  cluster:

$$\text{EE}(\text{M}@\text{Si}_8^n) = E(\text{Si}_8, \text{lowest isomer}) + E(\text{M}^n) - E(\text{M}@\text{Si}_8^n)$$

where  $E(X)$  is the total energy of species X.

All the doped silicon clusters we are considering have 34 electrons. A pertinent question is about the global minimum of the isovalent bare  $\text{Si}_8^{2-}$  cluster. Figure 4 presents the low-lying structures of this dianion. Its global minimum turns out to be a  $T_d$  structure with four rhombic faces. The  $D_{2d}$  bis-disphenoidal structure, which is predicted by Wade-Mingos rules for the 18

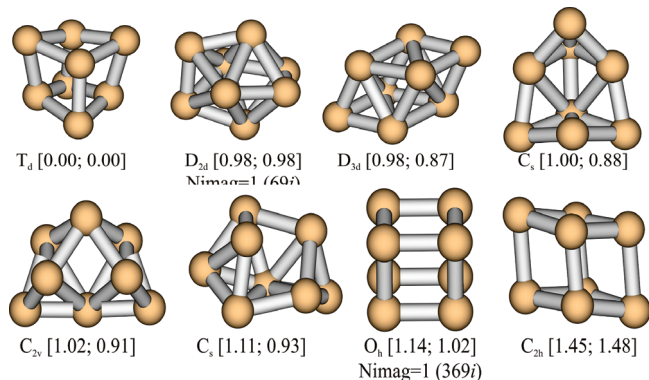


**Figure 4.** Low-lying isomers of  $\text{Si}_8^{2-}$ . Relative energies (eV) are obtained at the B3LYP/6-311+G(d) (left) and BP86/6-311+G(d) (right) levels.

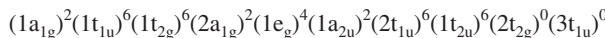
skeletal electrons ( $= 2n + 2$  for  $n = 8$ ), is located at 0.98 eV higher in energy than the global minimum. Moreover, a small imaginary frequency of  $69i \text{ cm}^{-1}$  found at the B3LYP/6-311+G(d) level for this bisdisphenoid indicates some degrees of fluxionality. Similar results were found for the heavier congener  $\text{Ge}_8^{2-}$  by King et al.<sup>26</sup> In the dianionic system, the cube exists as a transition structure with a significant imaginary frequency of  $369i \text{ cm}^{-1}$ .

**Electronic Structure of Be@Si<sub>8</sub>.** Let us now present a detailed analysis of the geometric and electronic structure of the neutral cube Be@Si<sub>8</sub>. The Be atom is situated at the center of the cube formed by eight Si atoms. The Be–Si bond distance is calculated to be 2.169 Å (BP86), and the Si–Si bonds of 2.505 Å are not particularly larger than 2.357 Å obtained at the same level of theory for the Si–Si single bond in disilane. This implies that the cube is rather strained. It has a significantly large HOMO–LUMO gap of 2.01 eV obtained by BP86 (or even higher value of 2.99 eV obtained by B3LYP), which suggests a certain kinetic stability.

The density of states (DOS) of a molecular system can be regarded as the energy spectrum of its molecular orbitals (MOs). The partial density of states (pDOS) is computed only from relevant atomic orbitals and shows the composition of the MOs involved. The plots for total and pDOSs of the Be@Si<sub>8</sub> cube displayed in Figure 5 illustrate a clear picture of the electronic shells. This figure also shows the shape, notation, and quantitative energy ordering of the shell orbitals. According to the shape of the MOs involved, we derive the occupied shell sequence as follows:  $1S^2 1P^6 1D^6 2S^2 1D^4 1F^2 2P^6 1F^6$ . This is the shell performance of the valence electronic configuration of the cubic Be@Si<sub>8</sub> obtained by quantum chemical calculations at the BP86/6-311+G(d) level:

**TABLE 1: Geometrical Parameters (Å), HOMO (H, eV), LUMO (L, eV) Energies, HOMO–LUMO Gaps (H–L, eV), Mulliken Atomic Charges (electron), and Embedding Energies (EE, eV) of the 34-Electron Cubic Silicon Systems Considered (BP86/6-311+G(d))**

system	character	$r(\text{Si–Si})$	$r(\text{Si–M})$	H	L	H–L gap	charge on dopant	charge on each Si atom	EE
$\text{Si}_8^{2-}$	saddle point	2.409							
$\text{Li}@{\text{Si}_8}^-$	local minimum	2.534	2.195	-1.84	0.56	1.90	-1.95	+0.22	1.71
$\text{Be}@{\text{Si}_8}$	global minimum	2.505	2.169	-5.80	-3.79	2.01	+0.54	-0.07	3.01
$\text{B}@{\text{Si}_8}^+$	global minimum	2.471	2.140	-9.98	-7.83	2.15	+3.51	-0.31	7.87
$\text{C}@{\text{Si}_8}^{2+}$	global minimum	2.462	2.132	-14.26	-12.02	2.24	+1.52	+0.06	24.87
$\text{N}@{\text{Si}_8}^{3+}$	local minimum	2.496	2.161	-18.52	-16.35	2.17	-0.57	+0.45	63.25
$\text{O}@{\text{Si}_8}^{4+}$	local minimum	2.580	2.235	-22.58	-21.44	1.14	-1.12	+0.64	132.35



The orbitals involved can briefly be described as follows:

(i) The highest symmetry combination ( $1a_{1g}$ ) of the 3s-AOs of eight Si atoms gives rise to the 1S orbital of the cubic cage, which further interacts with the 2s-AO (Be) to form the bonding shell orbitals 1S ( $1a_{1g}$ ) and 2S ( $2a_{1g}$ ). The former is localized and lies deeper than the other valence MOs; therefore, it is regarded as a localized state while the latter describes the interaction between Be and the cubic Si cage.

(ii) The lower symmetry combinations ( $1t_{1u}$ ) of the 3s-AOs of Si atoms form the shell orbital 1P, where the 3p-AOs (Si) and 2p-AOs (Be) also contribute, but at a lesser extent. Therefore, these MOs should be responsible for the Si–Si  $\sigma$  bonds and are delocalized over the whole cage.

(iii) The  $1t_{2g}$  combinations of 3s-AOs of Si atoms have the shape of  $1D_{xy}$ ,  $1D_{xz}$ ,  $1D_{yz}$  orbitals and actually become the lower subshells of the cluster 1D shell orbital, and are also delocalized over the whole cage. It is known that the 1D level is split into two sublevels in a cubic crystal field ( $O_h$  symmetry). The lower-energy sublevel, namely  $t_{2g}$ , includes three orbitals  $1D_{xy}$ ,  $1D_{xz}$ , and  $1D_{yz}$ , and the higher one,  $e_g$ , includes  $1D_{z^2-x^2}$  and  $1D_{y^2-x^2}$  (these orbitals correspond to  $1D_{z^2-y^2}$  and  $1D_{x^2}$  in perfectly spherical field). In this case, the splitting energy of 2.5 eV is quite large. The latter are mainly composed of 3p-AOs of the Si atoms.

(iv) The subsequent MO ( $1a_{2u}$ ) is the lowest symmetric combination of 3s-AOs of Si atoms and has the shape of  $1F_{xyz}$  shell orbital.

(v) The  $2t_{1u}$  MOs are bonding combinations between 2p-AOs (Be) and 3s-AOs (Si) and appear as 2P shell orbitals. They are indeed responsible for a bonding interaction between the dopant and the Si cage and fully occupied by 6 electrons.

(vi) The  $1t_{2u}$  MOs are mainly composed of 3p-AOs (Si), and look like the  $1F_{x(z^2-y^2)}$ ,  $1F_{y(z^2-x^2)}$ ,  $1F_{z(x^2-y^2)}$  shell orbitals.

In summary, the  $\text{Be}@\text{Si}_8$  cluster, which constitutes the first neutral Si cluster found to have a cubic form, is characterized by an electronic closed shell of  $1S^2 1P^6 1D^6 2S^2 1D^4 1F^2 2P^6 1F^6$ . The 2S shell goes in between the two subshells of 1D, and the 2P shell goes in between the subshells of 1F. As for a general extension, the separation between shell orbitals really depends on the shape, charge of cluster, and nature of dopant. The 17

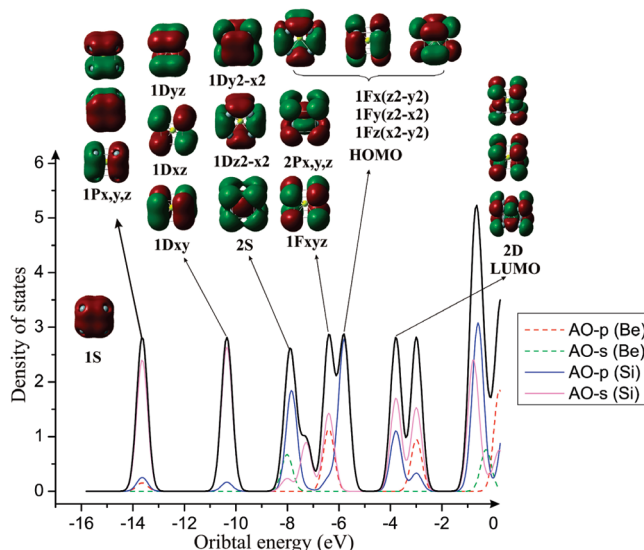


**Figure 5.** Total (black solid line) and partial (colored lines) DOSs of the  $\text{Be}@\text{Si}_8$  cube.

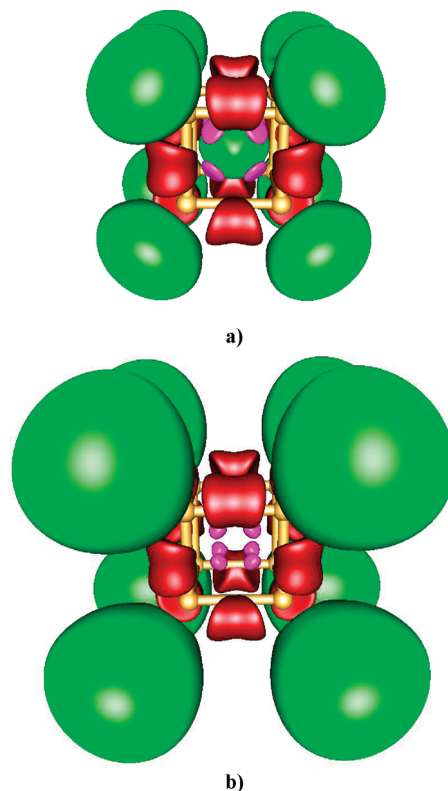


**Figure 6.** pELI-D for the cubic structure of  $\text{Be}@\text{Si}_8$  (a) and  $\text{Si}_8^{2-}$  (b). Pink color displays the 0.25-localization domains for 1S shell orbital. Red color displays the 1.5-localization domains for summation over 12 MOs (1P, 1D shell orbitals and 6MOs of 1F shell). Green color displays the 0.75-localization for summation over 4 MOs (2S and 2P shell orbitals).

occupied valence MOs can therefore be divided into three main groups, namely, (a) the 1S MO regarded as the localized valence state; (b) the 12 MOs ( $1P_{x,y,z}$ ,  $1D$ ,  $1F_{xyz}$ ,  $1F_{x(z^2-y^2)}$ ,  $1F_{y(z^2-x^2)}$  and  $1F_{z(x^2-y^2)}$ ) describing the Si–Si  $\sigma$  bonds; and (c) the 4 MOs (2S and 3 MOs of  $2P_{x,y,z}$  nature) describing the interaction between Be and Si cage.

The electronic structure of  $\text{Be}@\text{Si}_8$  is further analyzed using partial ELI-D contributions that are presented in Figure 6a. Three different colors are used to describe the pELI-D plotted for three MO groups. The pink-colored domains arising from 1S shell orbital are strongly localized on the connections between Be center and Si atoms. The red-colored localization domains, which are located in the middle of Si–Si bonds, arise from the pELI-D of the second group of 12 MOs. The pELI-D picture confirms the aforementioned assignment that these orbitals, namely  $1t_{1u}$ ,  $1t_{2g}$ ,  $1e_g$ ,  $1a_{2u}$ , and  $1t_{2u}$ , are responsible for the Si–Si  $\sigma$  bonds. These localization domains of  $\text{Be}@\text{Si}_8$  are very similar to those of the cubic dianion  $\text{Si}_8^{2-}$  shown in Figure 6b. This means that the red domains mainly arise from AOs of Si atoms, and the dopant hardly plays any role in these localization domains. On the other hand, the green domains, that are computed over the third group of four MOs (2S and 2P shell orbitals) describing the interactions between Be and the cage, include one domain centered in the middle and eight domains pointing outward the cage in the direction of Be–Si bonds. These domains are strongly delocalized over, both inside and outside, the whole cage. The green domains in the case of dianion  $\text{Si}_8^{2-}$  only appear outside the cage and are much larger than those of  $\text{Be}@\text{Si}_8$ . Therefore, the presence of Be at the cage center attracts some electron density into the center and increases the electron density around the cube (because the volumes of

**TABLE 2: Occupied Shell Sequences of the Cubic 34-Electron Systems**

system	1S	1P	1D	1F	1D	2S	1F	2P	electronic (orbital) configuration
$\text{Si}_8^{2-}$	1S	1P	1D	1F	1D	2S	1F	2P	$(1\text{a}_{1g})^2(1\text{t}_{1u})^6(1\text{t}_{2g})^6(1\text{a}_{2u})^2(1\text{e}_g)^4(2\text{a}_{1g})^2(1\text{t}_{2u})^6(2\text{t}_{1u})^6$
$\text{Li}@\text{Si}_8^-$	1S	1P	1D	1D	1F	2S	2P	1F	$(1\text{a}_{1g})^2(1\text{t}_{1u})^6(1\text{t}_{2g})^6(1\text{e}_g)^4(1\text{a}_{2u})^2(2\text{a}_{1g})^2(2\text{t}_{1u})^6(1\text{t}_{2u})^6$
$\text{Be}@\text{Si}_8$	1S	1P	1D	2S	1D	1F	2P	1F	$(1\text{a}_{1g})^2(1\text{t}_{1u})^6(1\text{t}_{2g})^6(1\text{e}_g)^4(1\text{a}_{2u})^2(2\text{a}_{1g})^2(2\text{t}_{1u})^6(1\text{t}_{2u})^6$
$\text{B}@\text{Si}_8^+$	1S	1P	1D	2S	1D	1F	2P	1F	$(1\text{a}_{1g})^2(1\text{t}_{1u})^6(1\text{t}_{2g})^6(1\text{e}_g)^4(1\text{a}_{2u})^2(2\text{a}_{1g})^2(1\text{t}_{2u})^6(1\text{t}_{2u})^6$
$\text{C}@\text{Si}_8^{2+}$	1S	1P	2S	1D	1D	2P	1F	1F	$(1\text{a}_{1g})^2(1\text{t}_{1u})^6(2\text{a}_{1g})^2(1\text{t}_{2g})^6(1\text{e}_g)^4(1\text{a}_{2u})^2(2\text{t}_{1u})^6(1\text{t}_{2u})^6$
$\text{N}@\text{Si}_8^{3+}$	1S	1P	2S	1D	2P	1D	1F	1F	$(1\text{a}_{1g})^2(1\text{t}_{1u})^6(2\text{a}_{1g})^2(1\text{t}_{2g})^6(2\text{t}_{1u})^6(1\text{e}_g)^4(1\text{a}_{2u})^2(1\text{t}_{2u})^6$
$\text{O}@\text{Si}_8^{4+}$	1S	1P	2S	1D	2P	1F	1D	1F	$(1\text{a}_{1g})^2(1\text{t}_{1u})^6(2\text{a}_{1g})^2(1\text{t}_{2g})^6(2\text{t}_{1u})^6(1\text{a}_{2u})^2(1\text{e}_g)^4(1\text{t}_{2u})^6$

the outward lobes are reduced). The fact that the green domains are distributed both inside and outside the cage but not along the Be–Si bonds refers to an ionic character of Be–Si bonds. The positive Mulliken net charge of 0.54 electron on Be is expected to contribute somewhat to a electrostatic stabilization of the electronic clouds along the dangling lobes of Si atoms.

From the above analysis, we would propose a chemical bonding model for the cubic Be@Si<sub>8</sub> cluster as follows: (1) each Si atom has four lobes of sp<sup>3</sup> hybridization; (2) three of them make three covalent σ bonds with other Si atoms, in such a way that there are 12 σ bonds in this cube (corresponding to 24 electrons); and (3) the fourth lobe makes an ionic bond with Be atom. The eight electrons distributed on 2S and 2P shell orbitals are found inside and outside of the cage, and delocalized over the entire cluster; and (4) the positive charge at the cube center tends to stabilize the dangling lobes of Si atoms by electrostatic forces.

**Electronic Structure of the Cubic Second-row Element Doped Silicon Clusters.** In order to verify the validity of the above chemical bonding model, we carry out the same electronic analysis for the other 34-electron cubic systems including Si<sub>8</sub><sup>2-</sup>, Li@Si<sub>8</sub><sup>-</sup>, Be@Si<sub>8</sub>, B@Si<sub>8</sub><sup>+</sup>, C@Si<sub>8</sub><sup>2+</sup>, N@Si<sub>8</sub><sup>3+</sup>, and O@Si<sub>8</sub><sup>4+</sup>. The main results obtained for these systems such as geometrical parameters, frontier orbital energies and the gap between them, and atomic net charges are summarized in Table 1. Their electron configurations and the corresponding occupied shell sequences are tabulated in Table 2. Their total densities of states are compared in Figure 7.

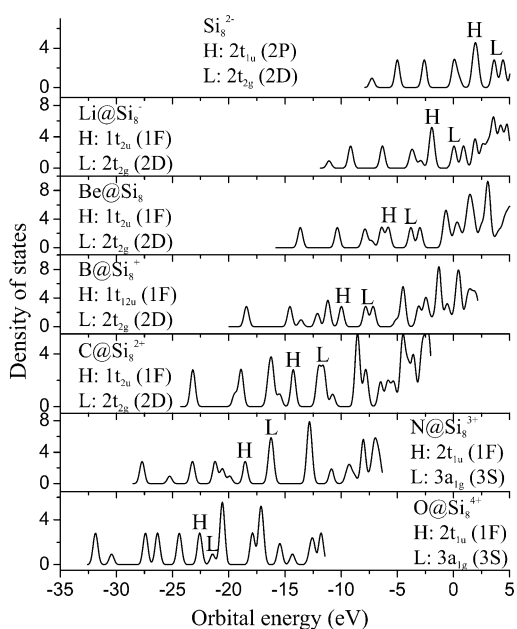


**Figure 7.** Total densities of states of the 34-electron cubes: Si<sub>8</sub><sup>2-</sup>, Li@Si<sub>8</sub><sup>-</sup>, Be@Si<sub>8</sub>, B@Si<sub>8</sub><sup>+</sup>, C@Si<sub>8</sub><sup>2+</sup>, N@Si<sub>8</sub><sup>3+</sup>, and O@Si<sub>8</sub><sup>4+</sup>.

To investigate the importance of a full occupancy of shell orbitals, we first look at the bare silicon dianion Si<sub>8</sub><sup>2-</sup>, which is isovalent with Be@Si<sub>8</sub> having each 34 valence electrons. The situation is described in Figure 8. Addition of two excess electrons in the lowest-lying Si<sub>8</sub> isomer is an exothermic process by −1.03 eV. The resulting dianion exhibits a D<sub>3d</sub> geometry. The Si<sub>8</sub><sup>2-</sup> cube under O<sub>h</sub> symmetry is characterized as a transition structure whose transition vector (imaginary A<sub>2u</sub> mode) describes the asymmetric movements of Si atoms inward and outward of the center. The other Si<sub>8</sub><sup>2-</sup> isomer connected by the cubic transition structure turns out to be the global minimum of this dianion with a T<sub>d</sub> symmetry. Thus, the fact is that only a full occupancy of the shell orbitals is not sufficient to stabilize the cube.

In addition, the global minimum T<sub>d</sub>, which has longer Si–Si bonds than those of the cube, becomes now a cage with six faces. Accordingly, relaxation from the cube just transforms the cube's squares into bent rhombuses of the T<sub>d</sub> structure. And all the Si–Si–Si bond angles of the T<sub>d</sub> structure amount to 106.6°, which is a typical bond angle of sp<sup>3</sup> hybridization. Hence, the Si atoms apparently favor an sp<sup>3</sup> hybridization, and by adding two excess electrons, the bare Si<sub>8</sub><sup>2-</sup> cube does exist as a stationary point, but not yet as a local energy minimum. This suggests that by putting an atom inside, which satisfies the 34-electron requirement, it is possible to stabilize the strained silicon cube. This is indeed the case when doping it with second-row elements.

However only in the cases of Be, B, and C dopants, the cubic structures become global minima, whereas in the rest they are rather local minima. A question is thus what makes the difference between them. Inspecting their atomic charges, we

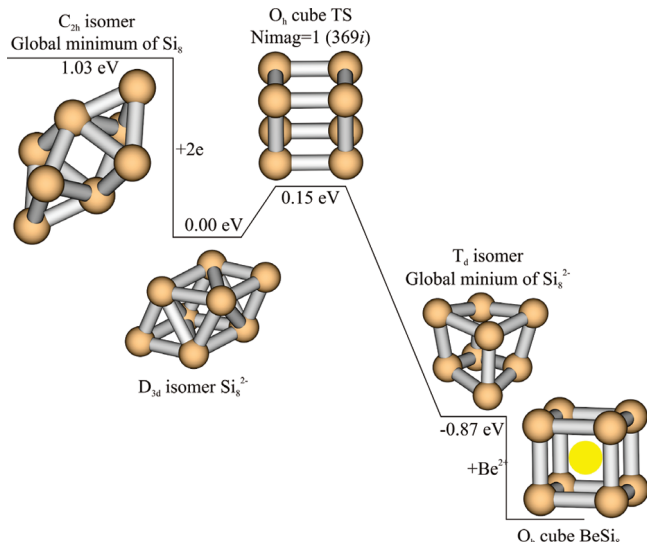


**Figure 8.** Schematic energy profile describing the formation of the neutral cubic beryllium-doped silicon cluster. Relative energies are from BP86/6-311+G(d) calculations.

find that the Be, B, or C element is substantially positively charged (0.54, 3.51, and 1.52 electrons, respectively), while it is negatively charged in other cases. Hence, the presence of a positive charge at the cube center contributes to stabilize the fourth lobe of Si atoms. Moreover, the cubic structure of  $\text{BSi}_8^+$  is much lower in energy than its other isomeric forms, whereas it is not the case for  $\text{BeSi}_8$  and  $\text{CSi}_8^{2+}$ . This special behavior of  $\text{BSi}_8^+$  is related to the large positive charge (3.51 electron) of B atom as compared to those of Be and C atoms. The positive charge at the center is another key factor for the existence of the cube.

The DOS or MO energy spectra of seven 34-electron cubic systems considered ( $\text{Si}_8^{2-}$ ,  $\text{Li@Si}_8^-$ ,  $\text{Be@Si}_8$ ,  $\text{B@Si}_8^+$ ,  $\text{C@Si}_8^{2+}$ ,  $\text{N@Si}_8^{3+}$ , and  $\text{O@Si}_8^{4+}$ ) are compared in Figure 7. They have similar occupancy of shell orbitals including 1S, 1P, 1D, 1F<sub>xyz</sub>, 1F(t<sub>2g</sub>), 2S, and 2P, but the shell sequences differ slightly from each other. Table 2 and Figure 7 provide a clear picture that the shell sequence strongly depends on the nature of dopant and the charge of the system. As the atomic number of dopant (and thereby the positive charge of the system) increases, the resulting MO energies are consistently lowered. Especially, the shell orbitals 2S and 2P, which describe the interaction between dopant and cage, are energetically lowered. In other words, they are more stabilized in going from Li to O as dopant. For example, the 2P shell orbital of  $\text{Si}_8^{2-}$  corresponds to the HOMO, but it moves one energy level lower upon doping of Li, Be, and B atoms, two levels lower following doping of C atom, and three levels lower upon doping of N and O atoms. The reason for such a stabilization of 2S and 2P orbitals is an interaction of the dopant's 2s and 2p orbitals with the shell orbitals of the  $\text{Si}_8^{2-}$  cube, which appears to play a crucial role.

**Aromaticity and Electron Counting Rule.** Due to the existence of delocalized electrons that involve in the interaction between dopant and cubic cage, it is worth considering the clusters in terms of aromaticity. Whereas the classical  $(4n + 2)$  rule is widely applied for the aromaticity of planar molecules,<sup>27</sup> the  $2(n + 1)^2$  Hirsch rule,<sup>28</sup> which is a counterpart of Hückel rule, is applicable for spherical systems.<sup>29</sup>

The Hirsch way of counting electrons<sup>28</sup> points out that the maximum spherical aromaticity occurs in icosahedral fullerenes when the valence  $\pi$ -shells are completely filled with  $2(n + 1)^2$  electrons. Later, Chen et al.<sup>30</sup> also demonstrated that the latter also holds for the spherical aromaticity of less symmetric fullerenes. We now probe as to whether any of these rules are applicable for the silicon cubes considered.

As discussed above, the electron densities of the 2S and 2P shell orbitals illustrated by green domains in Figure 6 are spherically delocalized, while the others are localized on the Si framework. Thus, the 2S and 2P shells filled by 8 electrons refer to a certain spherical aromaticity according to the  $2(n + 1)^2$  electrons (with  $n = 1$ ). However, we would notice that the separation of green domains defines a new topology of aromaticity.

The electron counting rule often counts the number of delocalized electrons. For example, in the case of lithium and sodium clusters, they are valence electrons. In the case of carbon fullerenes, they involve  $\pi$ -electrons. In the present cubic silicon clusters, they are electrons on the 2S and 2P shells which have both s and p character (c.f., PDOS plot in Figure 5). In general, these MOs are not the HOMO and they energetically lie in between other localized orbitals (c.f., Table 2). All the shell orbitals having principal quantum number  $N = 1$  are localized. Although this finding cannot easily be generalized, it shows that if the shell orbitals having principal quantum number  $N > 1$  are

filled, the molecule exhibits a maximal aromatic character. Hence, the cubic doped silicon clusters can be regarded as the 8 delocalized electron systems. This constitutes an important driving factor for their thermodynamic stability.

Let us consider the systems with larger number of electrons to support this concept. The LUMO of the  $\text{Li@Si}_8^-$ ,  $\text{Be@Si}_8$ ,  $\text{B@Si}_8^+$ , and  $\text{C@Si}_8^{2+}$  minima is a  $2t_{2g}$  orbital, or a 2D shell orbital. In principle, when this shell are filled (for example in  $\text{C@Si}_8^{4-}$ ) the cube could be formed. However, this is not the case here. Also the LUMO of  $\text{N@Si}_8^{3+}$  or  $\text{O@Si}_8^{4+}$  is a  $3a_{1g}$  orbital, corresponding to a 3S shell orbital. Again, when the LUMO is filled (for example in  $\text{O@Si}_8^{2+}$ ) a cubic structure is not formed either. What is the reason for such a behavior? When adding 6 excess electrons on the 2D shell orbitals, or 2 extra electrons on the 3S shell orbital, which are responsible for the dopant-cage interaction, we end up with either 14 or 10 delocalized electrons, respectively, which do not obey the Hirsch rule, and are therefore nonaromatic. It is obvious that the cubes that are 8-electrons systems, feature a distinct type of spherical aromatic character.

## Concluding Remarks

In this theoretical contribution, we rationalize the chemical bonding of the cubic doped silicon clusters  $\text{M@Si}_8$ , which can be summarized as follows:

(i) The system needs to have the filled shell orbitals with 34 valence electrons to be able to exist in a cubic form.

(ii) A cubic isomer becomes the global energy minimum if there is a positive charge at the cube center and a maximal spherical aromaticity such as in the cases of  $\text{Be@Si}_8$ ,  $\text{B@Si}_8^+$ ,  $\text{C@Si}_8^{2+}$ .

(iii) In the cube, each Si atom has four lobes of  $\text{sp}^3$  hybridization in which three lobes make three covalent  $\sigma$  bonds with other Si atoms, and the fourth lobe makes a chemical bond with the dopant atom.

(iv) The DOS and pELI-D analyses in combining with the PSM open a way of classifying electrons in the doped silicon clusters. The shell orbitals with the principal quantum number  $N = 1$  (1S, 1P, 1D, and 1F) are localized and responsible for the Si–Si  $\sigma$  bonds (except 1S shell orbital), and the shell orbitals with  $N > 2$  (2S and 2P) delocalized and responsible for the dopant–Si cage interaction.

(v) The number of delocalized electrons on 2S and 2P shell orbitals obeys the Hirsch rule. This becomes one of the driving factors for forming cube. For a simpler electron count, the stable cubic clusters can be regarded as 8-electron systems.

**Acknowledgment.** The authors are indebted to the KULEuven Research Council (GOA, IDO and IUAP programs), and the Flemish Fund for Scientific Research (FWO-Vlaanderen) for continuing support. MTN thanks the ICST of HoChiMinh City for supporting his stays in Vietnam.

**Supporting Information Available:** The Cartesian coordinates of the optimized structures shown in Figures 1–4. This materials is available free of charge via the Internet at <http://pubs.acs.org>.

## References and Notes

- Tang, M.; Lu, W.; Wang, C. Z.; Ho, K. M. *Chem. Phys. Lett.* **2003**, 377, 431–418.
- Zhu, X.; Zeng, X. C. *J. Chem. Phys.* **2003**, 118, 3558–3569.
- Lyon, J. T.; Gruene, P.; Fielicke, A.; Meijer, G.; Janssens, E.; Claes, P.; Lievens, P. *J. Am. Chem. Soc.* **2009**, 131, 1115–1121.

- (4) Levine, I. N. *Quantum Chemistry*, 5th ed.; Prentice Hall: 2000; p 52.
- (5) Gruene, P.; Fielicke, A.; Meijer, G.; Janssens, E.; Ngan, V. T.; Nguyen, M. T.; Lievens, P. *ChemPhysChem* **2008**, *9*, 703–706.
- (6) Fan, H.; Yang, J.; Lu, W.; Ning, H.; Zhang, Q. *J. Phys. Chem. A* **2010**, *114*, 1218–1223.
- (7) Kumar, V. *Comput. Mater. Sci.* **2006**, *36*, 1–11.
- (8) de Heer, W. A. *Rev. Mod. Phys.* **1993**, *65*, 611–676.
- (9) Brack, M. *Rev. Mod. Phys.* **1993**, *65*, 677–730.
- (10) Neukermans, S.; Janssens, E.; Chen, Z. F.; Silverans, R. E.; Schleyer, P. v. R.; Lievens, P. *Phys. Rev. Lett.* **2004**, *92*, 163401.
- (11) Janssens, E.; Neukermans, S.; Lievens, P. *Curr. Opin. Solid. State Mater. Sci.* **2004**, *8*, 185–193.
- (12) Holtzl, T.; Lievens, P.; Veszpremi, T.; Nguyen, M. T. *J. Phys. Chem. C* **2009**, *113*, 21016–21018.
- (13) Reveles, J. U.; Khanna, S. N. *Phys. Rev. B* **2006**, *74*, 035435.
- (14) Hiura, H.; Miyazaki, T.; Kanayama, T. *Phys. Rev. Lett.* **2001**, *86*, 1733–1736.
- (15) Khanna, S. N.; Rao, B. K.; Jena, P. *Phys. Rev. Lett.* **2002**, *89*, 016803.
- (16) Kohout, M.; Wagner, F. R.; Grin, Y. *Int. J. Quantum Chem.* **2006**, *106*, 1499–1507.
- (17) Wagner, F. R.; Bezugly, V.; Kohout, M.; Grin, Y. *Chem.—Eur. J.* **2007**, *13*, 5724–5741.
- (18) Holtzl, T.; Janssens, E.; Veldeman, N.; Veszpremi, T.; Lievens, P.; Nguyen, M. T. *ChemPhysChem* **2008**, *9*, 833–838.
- (19) Lin, L.; Holtzl, T.; Gruene, P.; Claes, P.; Meijer, G.; Fielicke, A.; Lievens, P.; Nguyen, M. T. *ChemPhysChem* **2008**, *9*, 2471–2474.
- (20) Kohout, M. *DGrid, version 4.2*; Max-Planck Institut für Chemische Physik und Fester Stoffe: Dresden, 2006.
- (21) Becke, A. D. *J. Chem. Phys.* **1993**, *98*, 5648–5652.
- (22) Lee, C.; Yang, W.; Parr, R. G. *Phys. Rev. B* **1988**, *37*, 785–789.
- (23) Becke, A. D. *Phys. Rev. A* **1988**, *38*, 3098–3100.
- (24) Perdew, J. P. *Phys. Rev. B* **1986**, *33*, 8822–8824.
- (25) Frisch, M. J.; Trucks, G. W.; Schlegel, H. B.; Scuseria, G. E.; Robb, M. A.; Cheeseman, J. R.; Montgomery, Jr., J. A.; Vreven, T.; Kudin, K. N.; Burant, J. C.; Millam, J. M.; Iyengar, S. S.; Tomasi, J.; Barone, V.; Mennucci, B.; Cossi, M.; Scalmani, G.; Rega, N.; Petersson, G. A.; Nakatsuji, H.; Hada, M.; Ehara, M.; Toyota, K.; Fukuda, R.; Hasegawa, J.; Ishida, M.; Nakajima, T.; Honda, Y.; Kitao, O.; Nakai, H.; Klene, M.; Li, X.; Knox, J. E.; Hratchian, H. P.; Cross, J. B.; Bakken, V.; Adamo, C.; Jaramillo, J.; Gomperts, R.; Stratmann, R. E.; Yazyev, O.; Austin, A. J.; Cammi, R.; Pomelli, C.; Ochterski, J. W.; Ayala, P. Y.; Morokuma, K.; Voth, G. A.; Salvador, P.; Dannenberg, J. J.; Zakrzewski, V. G.; Dapprich, S.; Daniels, A. D.; Strain, M. C.; Farkas, O.; Malick, D. K.; Rabuck, A. D.; Raghavachari, K.; Foresman, J. B.; Ortiz, J. V.; Cui, Q.; Baboul, A. G.; Clifford, S.; Cioslowski, J.; Stefanov, B. B.; Liu, G.; Liashenko, A.; Piskorz, P.; Komaromi, I.; Martin, R. L.; Fox, D. J.; Keith, T.; Al-Laham, M. A.; Peng, C. Y.; Nanayakkara, A.; Challacombe, M.; Gill, P. M. W.; Johnson, B.; Chen, W.; Wong, M. W.; Gonzalez, C.; Pople, J. A.; Gaussian 03, revision E.01; Gaussian, Inc.: Wallingford CT, 2004.
- (26) King, R. B.; Silaghi-Dumitrescu, I.; Lupan, A. *Dalton Trans.* **2005**, 1858–1864.
- (27) Höltzl, T.; Janssens, E.; Veldeman, N.; Veszprémi, T.; Lievens, P.; Nguyen, M. T. *Chem. Phys. Chem.* **2008**, *8*, 33, 9.
- (28) Hirsch, A.; Chen, Z.; Jiao, H. *Angew. Chem., Int. Ed.* **2000**, *39*, 3915.
- (29) Veldeman, N.; Höltzl, T.; Neukermans, S.; Veszprémi, T.; Lievens, P.; Nguyen, M. T. *Phys. Rev. A* **2007**, *76*, 011201(R).
- (30) Chen, Z.; Jiao, H.; Hirsch, A.; Thiel, W. *J. Mol. Model.* **2001**, *7*, 161–163.

JP103180Y